ORIGINAL ARTICLE

DOI: https://doi.org/10.18599/grs.2024.1.8 Russian Original 2024. Vol. 26. Is. 1. Pp. 100–108

Influence of Reservoir Microstructure on the State of Residual Oil According to Nuclear Magnetic Resonance (NMR) Spectroscopy

Mo Jiali[1], N.N. Mikhailov[1,2], Wang Hengyang[3]*

[1]*National University of Oil and Gas "Gubkin University", Moscow, Russian Federation*

[2]*Institute of Oil and Gas Problems of the Russian Academy of Sciences, Moscow, Russian Federation*

[3]*Sinopec Research Institute of Petroleum Engineering, Beijing, China*

Abstract. The influence of core properties on the state of residual oil in the process of oil displacement by water at the micro level is investigated. The pore size distribution, core permeability, dynamics and morphology of residual oil were studied. The analysis of the available experimental approaches to the study of the properties of the core and residual oil in the core samples showed that the existing methods do not provide complete information about the studied parameters. To solve these problems, it is proposed to use a combination of innovative relaxation-diffusion spectroscopy technology of nuclear magnetic resonance with traditional technology. A combination of mercury injection and nuclear magnetic resonance is used to measure the pore size distribution. The core permeability was determined using the nuclear magnetic resonance method. Two-dimensional nuclear magnetic resonance spectroscopy makes it possible to study the microscopic state of residual oil in an undisturbed core during the displacement process. With the help of the proposed methodology, a core study of the Shengli Oil Field in China was carried out. Pore size distributions were obtained, permeability and residual oil saturation at different stages of displacement were studied. Four types of residual oil are distinguished: strip-shaped (island), film, mesh, continuous. The influence of permeability on the fraction content of different types of residual oil in the process of displacement is shown. The research results demonstrate the influence of the pore space structure and wettability on the state of residual oil.

Keywords: types of residual oil, pore space structure, relaxation-diffusion two-dimensional NMR spectroscopy

Recommended citation: Jiali Mo, Mikhailov N.N., Hengyang Wang (2024). Influence of Reservoir Microstructure on the State of Residual Oil According to Nuclear Magnetic Resonance (NMR) Spectroscopy. *Georesursy = Georesources*, 26(1), pp. 100–108. https://doi.org/10.18599/grs.2024.1.8

Introduction

Combination of mercury injection method and nuclear magnetic resonance

The structure of a reservoir's pore space is critical to assessing development potential, oil recovery and productivity (Mikhailov, 1992).

Pore size distribution is one of the main parameters in the quantification and characterization of pore structures. Test methods can be divided into image analysis methods (slices, scanning electron microscopy and CT scan), fluid penetration methods (mercury injection and gas adsorption) and non-fluid penetration methods (nuclear magnetic resonance (NMR), etc.). The advantages of NMR technology are ease of operation, low cost and no damage to the sample being measured. This technology is widely used in studying the pore structure and surface properties of reservoir rocks, which allows us to study all pores in rock samples. A parameter for studying pore space is the transverse relaxation time (T_2), the spectrum of which reflects the trend in the volumetric distribution of pores of various sizes (Arns, 2004; Tchistiakov et al., 2022).

As a rule, the longer the transverse relaxation time, the larger the pore radius; there is a proportional relationship between them, but the transverse relaxation time is not directly related to the absolute pore size. If the correlation between transverse relaxation time and pore radius is established, the T_2 nuclear magnetic resonance spectrum can be converted into a radius distribution and a precise quantification of the overall pore structure of reservoir rocks can be assessed.

Currently, many scientists use mercury injection experiment data to calibrate the T_2 spectrum and establish

*Corresponding author: Nikolai N. Mikhailov
e-mail: folko200@mail.ru

the correlation between transverse relaxation time and pore radius.

NMR analysis of reservoir properties and fluid characteristics is based on studying the response of hydrogen nuclei in the studied environment to a magnetic field. The experiment usually uses low magnetic field strength. When the experiment uses a low magnetic field strength the NMR signal produced by the organic matter in the rock matrix is very weak, so the proton information in the skeleton can be neglected.

The magnetic field interacts with the spins of the hydrogen nuclei and produces a measurable signal reflected as amplitudes of varying magnitude, also known as a relaxation time. NMR relaxation time is mainly divided into longitudinal relaxation time (T_1) and transverse relaxation time (T_2). Measurements of these two parameters provide approximate information about the reservoir. However, transverse relaxation (T_2) measurement is predominantly used in laboratory studies due to its simplicity and efficiency. In this paper, only the transverse relaxation time (T_2) NMR spectrum is analyzed.

Structure of the measured transverse relaxation time

Transverse relaxation is affected by three different relaxation mechanisms: free relaxation (T_{2b}), surface relaxation (T_{2s}) and diffusion relaxation (T_{2d}), which are related by the following relationship (Kleinberg et al., 1993; Sulucarnain et al., 2012):

$$\frac{1}{T_2}=\frac{1}{T_{2s}}+\frac{1}{T_{2b}}+\frac{1}{T_{2d}}. \quad (1)$$

Since the pore size of the collector is very small, surface relaxation plays an important role. Free relaxation is mainly determined by the physical properties of the fluid. Diffusion relaxation is caused by the self-diffusion motion of hydrogen-containing molecules in a gradient magnetic field.

In this study, a gradient field was not created or used (a low internal gradient and a uniform magnetic field were maintained). The complete pulse sequence, consisting of an initial 90° pulse and a long series of 180° pulses, is called a sequence (CPMG). The CPMG values were used in our experiment to minimize the influence of diffusion relaxation, so the T_{2d} value can be neglected, then equation 1 takes the form:

$$\frac{1}{T_2}=\frac{1}{T_{2s}}+\frac{1}{T_{2b}}. \quad (2)$$

For fluids with a large intrinsic relaxation time in free volume (water, light oil, etc.)

$$\frac{1}{T_{2b}}\ll\frac{\rho s}{V}, \quad (3)$$

Therefore, the surface relaxation time of the liquid (T_2) is determined by the value $\rho s/V$, which reflects the geometry of the intrapore structure and the distribution of oil and water in it.

$$\frac{1}{T_2}=\frac{1}{T_{2s}}=\rho\frac{S}{V}=\rho\frac{F}{r}, \quad (4)$$

where ρ is the surface relaxation coefficient, μm/ms, s/v is the ratio of the pore area to its volume, 1/μm.

$$T_2=\frac{1}{\rho}\frac{V}{S}=\frac{r}{\rho F}=\frac{r}{C}, \quad (5)$$

$$r=CT_2, \quad (6)$$

where F is the geometric shape coefficient; C is specific surface area of pores, $C=1/\rho F$, 1/μm; r is pore radius, μm.

The distribution of rock pore structure can be reflected by a high-pressure mercury intrusion curve. On this basis, the NMR T_2 relaxation time distribution can be converted into a pore throat radius distribution by combining NMR with mercury intrusion (Sun et al., 2017).

Technology for studying the structure of pore space using a combination of NMR and Mercury Intrusion Porosimetry

A reliable conversion factor is the basis for calculating the pore radius of reservoirs based on NMR relaxation time analysis.

Step 1. A high-order polynomial approximation is performed on the cumulative pore volume fraction curves corresponding to different pore radii in the high-pressure mercury injection experiment (Fig. 1a).

Step 2. To obtain cumulative pore volume fraction curves corresponding to different T_2, the T_2 signal intensity data and cumulative curves are normalized with increasing pore sizes. High order polynomials are also used to fit the curves to obtain the adaptation equation (Fig. 1b).

Step 3. Using regression equations based on data from the mercury injection experiment and the nuclear magnetic resonance experiment, the calculated pore radii and T_2 values corresponding to different cumulative pore volume fractions are determined. The obtained T_2 NMR spectrum is then compared with the values of pore radii determined during the high-pressure mercury injection experiment. The conversion factor (C) is obtained by adapting over a range of pore volume fraction (Fig. 1c).

Step 4. A generalized pore size distribution can be obtained by multiplying the T_2 spectrum obtained from the NMR experiment by the conversion factor C (Fig. 1d).

For convenience, the dimensionless parameter used is the total injected water coefficient, which is equal to the volume of water injected divided by the pore volume.

Core permeability

SDR model

The interconnected pores and fractures in the rock core form the filtration pore structure, and the pore sizes of this structure determine the permeability. Traditional

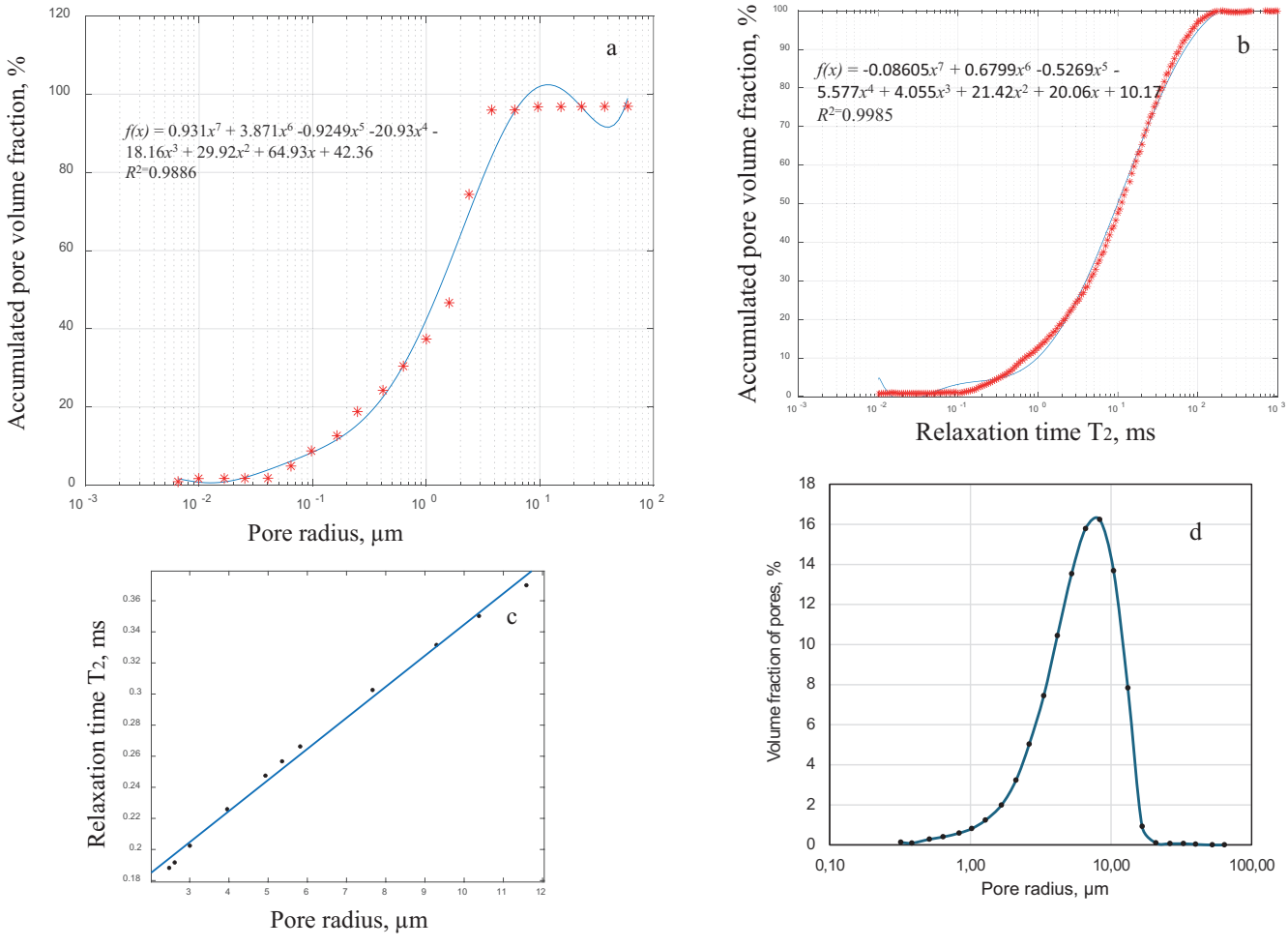

Fig. 1. Pore size distribution calibrated using NMR experiment and mercury injection of core samples: a – mercury injection; b – nuclear magnetic resonance experiment; c – conversion factor adaptation; d – calibrated pore size distribution

gas testing methods (pressure measurement or pulse confining pressure attenuation) and capillary pressure methods with mercury injection have certain limitations when studying reservoir permeability. Low-field NMR allows testing different fluid states and different fractions of pore space occupied by fluid in a core, which allows adequate calculation of permeability (Yan et al., 2021; Kenyon et al., 1988).

Currently, the calculation of absolute rock permeability (k) based on nuclear magnetic resonance technology is mainly based on the classical Coates model (Coates et al., 1991) and the SDR model (Kenyon, 1997), as well as extended models based on them.

The SDR model determines permeability from total porosity and geometric mean T_{2g}:

$$k = C_2 \varphi^4 T_{2g}^2, \quad (7)$$

where φ is porosity; C_2 is the permeability correction factor in the SDR model, associated with the type of formation, for the reservoir under consideration is equal to 4.285; T_{2g} is the geometric mean of relaxation times T_2.

The SDR model is based on the assumption that although pores of different sizes (different T_2 distributions) affect permeability in different ways, nevertheless the permeability of a sample can be calculated by averaging their distribution. Conventional reservoirs have a simple pore structure with a small ratio of pore radius to capillary radius, and the SDR model is generally used to obtain more accurate permeability values.

Experimental results and their discussion

The results of permeability determination by the above described technology are presented in Table 1. The studied core samples are characterized by medium and low porosity values and low permeability values.

The Shengli Oil Field in China is considered as an example. Fig. 2 shows the absolute permeability calculated by SDR model and the absolute permeability of the core measured experimentally. To ensure the validity of the experimental results, we measured the permeability of eight cores by nuclear magnetic resonance and gas permeability testing. It is clearly seen from Fig. 2 that the permeability values measured by the two methods are not significantly different. Thus, it can be concluded that the distribution of pore channels in the studied reservoirs is uniform, and the pore filtering structure is adequately described by the SDR model.

No. of core	Porosity, %	T_{2g}, ms	Absolute Permeability, $\times 10^{-3}$ μm ^{2}
1	11.6	79.02	0.0895
2	12.2	105.14	0.108
3	10.7	11.328	0.0088
4	10.45	57.703	0.0587
5	15.53	30.724	0.01854
6	16.03	37.326	0.02753
7	18.18	28.439	0.05787
8	15.61	11.168	0.00434

Table 1. Permeability of cores according to the experimental data

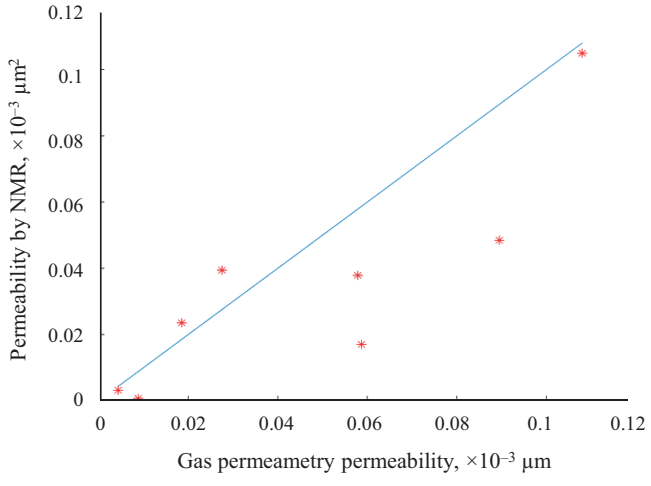

Fig. 2. Calculated (blue curve) and experimentally measured values of absolute permeability (marked with red asterisks) for the Shengli Field, China

Analysis of residual oil distribution during the displacement process

Residual oil, formed as a result of the displacement of oil by water during a laboratory experiment, is a complex dynamic structure (Mikhailov, 1992). Part of the residual oil is blocked by capillary forces and is conditionally mobile (i.e., immobile under the pressure gradients implemented in the experiment and mobile with increasing pressure gradient, as well as with temperature changes and possibly with the use of chemicals (surfactants, etc.)). The other part is motionless over a wide range of capillary number values (Melekhin, Mikhailov, 2017), it is represented by film and adsorbed oil, as well as oil of dead-end and low-flow pores of complex configuration.

Different types of residual oil have different properties and require different approaches to recover them. Standard laboratory experiments to determine residual oil saturation and displacement ratios do not allow differentiation of residual oil types and give only a generalized (integral) value.

Different types of residual oil have different properties and require different approaches to recover them. Standard laboratory experiments to determine residual oil saturation and the displacement factor do not allow differentiation of residual oil types and give only a generalized (integral) value.

Method of residual oil differentiation by type

Different states of residual oil have different effects on the water signal in the 2D NMR spectrum. The distribution of oil and water identified on the two-dimensional spectrum is more informative than on the relaxation spectrum (Mikhailov, 2011; Chen et al., 2006; Azizoglu et al., 2020). Thus, the advantages of two-dimensional relaxometry in studying the microscopic state of residual oil are obvious.

The bound water cutoff time T_c was determined by comparing diffusion-relaxation spectra of samples fully water-saturated and saturated with only bound water. The part of the two-dimensional spectrum where the relaxation time is longer than Tc represents the region of mobile water in the fully water-saturated core.

In the mobile water, the following were determined: the proportion of water (pld) with a relatively small diffusion coefficient ($< 1.5 \cdot 10^{-9}$ m^2/s, less than the normal value); the proportion of water (pcd) with a normal diffusion coefficient ($1.5 \cdot 10^{-9}$ to $2.5 \cdot 10^{-9}$ m^2/s); and the proportion of water (ped) with an abnormally large diffusion coefficient ($> 2.5 \cdot 10^{-9}$ m^2/s). The ratio of components with different diffusion coefficients is the basis for typification of residual oil (Fig. 3).

Based on images of the 2D diffusion-relaxation spectrum of a fully water-saturated core (Fig. 3a), the 2D spectrum during waterflooding (Fig. 3b) and the difference spectrum (Fig. 3c), taking into account the cut-off time of bound water (T_c) and the cut-off time of a typical oil film (T_o) it is possible to establish the difference spectrum characterizing the state of residual oil. As shown in Fig. 3c, the relaxation spectrum is divided into three parts along the ordinate (diffusion time): the part with relaxation time greater than T_o is the residual oil part, and the part with relaxation time less than T_c is the water part. The distribution of water diffusion coefficient in a typical water film and a typical oil film area is determined separately (Fig. 3c). Pld_{ow}, pcd_{ow} and ped_{ow} represent the fractions of restricted diffusion, normal diffusion coefficient and excess diffusion coefficient in a typical oil film area. On the 2D spectrum during the displacement process (using the values of T_c and T_o), the signal from water in the flooded pores is determined and the diffusion coefficient distribution of these pores is calculated.

In accordance with the distribution of diffusion coefficient at different relaxation time four types of residual oil will be distinguished: continuous, reticulated, strip and film, which allows to determine the share of each type in the total volume of residual oil.

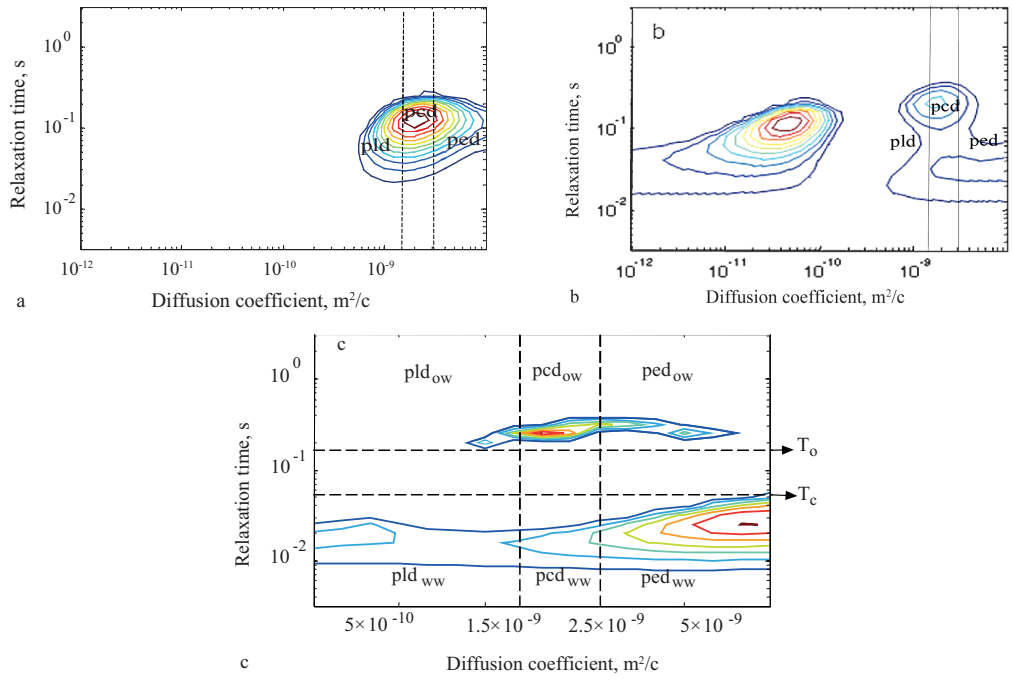

Fig. 3. Diffusion-relaxation two-dimensional spectrum: a – completely saturated water core; b – core during flooding; c – differences between areas (b–a) of water and oil saturation with a signal greater than 0

Criteria for typing residual oil

Two indices are used to quantitatively describe the state of the residual oil: the shape factor and the contact area factor.

Residual oil shape factor (G) is determined by the formula:

$$G = \frac{V}{S^{1,5}}, \quad (8)$$

where V is the isolated volume of residual oil; S is the surface area of the corresponding volume of residual oil.

From equation 8 follows: the smaller the shape factor, the larger the surface area of residual oil at the same volume and the more complex the geometric shape of the residual oil volume.

The residual oil contact area factor (C) is equal to the ratio of the residual oil contact area (S_{con}) to the total residual oil surface area (S_{tot}):

$$C = S_{con} / S_{tot}. \quad (9)$$

The residual oil contact area factor C reflects the relative structural ratio between residual oil and total pore surface: the smaller the contact area ratio, the smaller the proportion of residual oil on the pore surface and the higher the displacement ratio.

Other criteria characterizing the intra-pore geometry, obtained on the basis of the analysis of slides, are also applied: the number of pore channels in contact with the investigated volume of residual oil, as well as the ratio of the residual oil film thickness to the pore channel diameter.

The results of residual oil type classification are presented in Table 2.

Results and discussion

The experimental laboratory model is a set of reservoir cores taken from the studied field. When conducting experiments on microscopic displacement under various filtration conditions, several reservoir models with similar properties were used. As an example, Fig. 4 shows the results of the influence of the microscopic state of the oil remaining in the waterflooding process (sample H-4). Core porosity was 40.2%, core permeability was 4069 10^{-3} μm², and displacement rate was 0.2 ml/min.

The water relaxation spectra were measured at different injection ratios and then multiplied by the conversion factor obtained by a combination of mercury injection and nuclear magnetic resonance. Fig. 4 shows the pore volume fraction distribution obtained at the fully water-saturated state of the core. The pore volume fraction distribution curve obtained at full water saturation has a single pronounced peak with a large width. The predominant pore radius is approximately 10 μm, which characterizes the pore structure as simple with good connectivity between individual pores.

The distribution of water saturation in pores (Fig. 4) shows that with the increase of the total volume of injected water in units of pore volume, the water saturation of the core increases, and the curve of pore channel distribution also gradually shifts to the region of lower relaxation time. The pore distribution curve at a total injected water ratio of 1.2 or less corresponds to a bimodal distribution, with the modal value of the main peak being about 1 μm. This can be interpreted as during the waterflooding process, water preferentially

Residual oil type	Microscopic image	Classification criteria	Shape factor G	Contact area factor C
strip residual oil	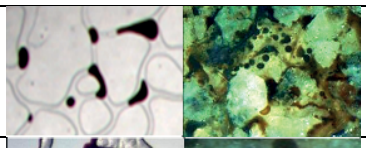	Number of pore channels = 1	$G > 0.03$	$0 < C < 1$
			$0.01 < G < 0.03$	$C < 0.45$ or $C > 0.6$
film residual oil	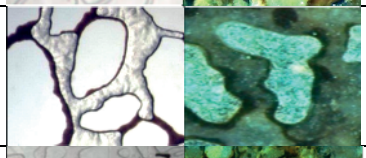	Film thickness less than 1/3 of pore diameter	$0.01 < G < 0.03$	$0.45 < C < 10.6$
reticulated residual oil	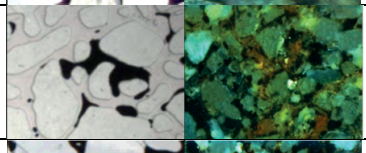	2 ≤ number of pore channels ≤ 5	$0.0007 < G < 0.01$	$0 < C < 11$
continuous residual oil	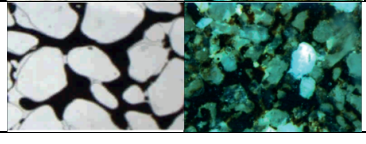	number of pore channels > 5	$G < 0.0007$	$0 < C < 11$

Table 2. Residual oil classification criteria

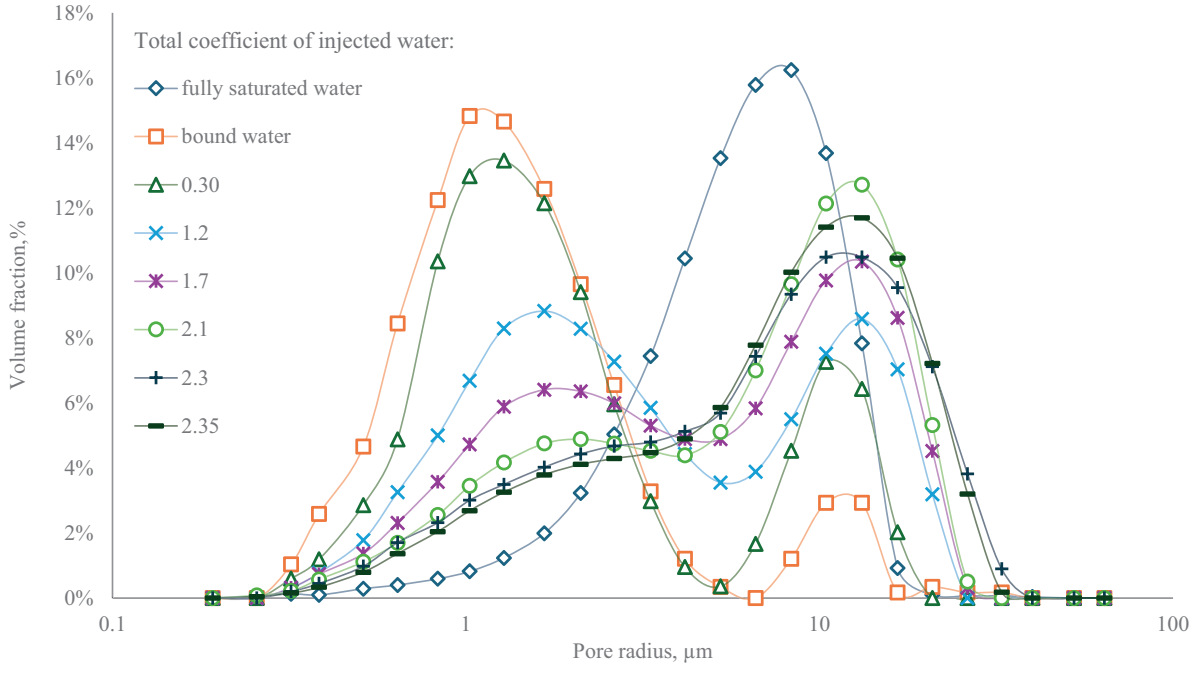

Fig. 4. Distribution curves of pore volume fraction during waterflooding for bound water and at different values of injected pore volume: 0.3; 1.2; 1.7; 2.1; 2.3; 2.3; 2.35 and for fully water-saturated cores

enters hydrophilic small pores or moves along the walls of hydrophilic large pores.

When the total injected water ratio increases from 1.2 to 2.35, the pore distribution curve gradually shifts: the bimodal distribution changes from 110 μm to 10 μm, with the proportion of small pores decreasing rapidly. This can be interpreted as at this stage water moves along the centers of macropores or along the walls of hydrophobic large pores. At this stage, a dominant system of water-filtering pores is formed. As a result, the displacement efficiency decreases, and the residual oil remains immobile and difficult to recover.

The change in the state of residual oil at different stages of watering indicates that mainly continuous oil is displaced. In the anhydrous stage, the oil is of a continuous type, and the residual oil is also of a continuous type, similar to natural oil. At the final stage of displacement (medium and high water cut), another type of residual oil predominates, and the proportion of reticulated and strip oil increases. At the high-water cut stage, the continuous oil changes to the reticulated. At the ultra-high water cut stage, the reticulated type prevails, as well as the strip type. The share of continuous residual oil sharply decreases (Fig. 5).

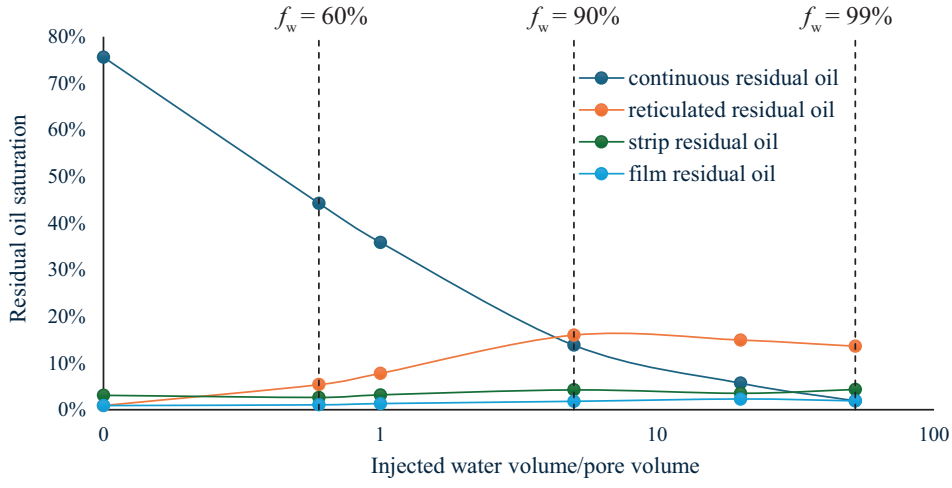

Fig. 5. Dynamics of residual oil saturation types depending on the volume of injected water (f_w – model water cut)

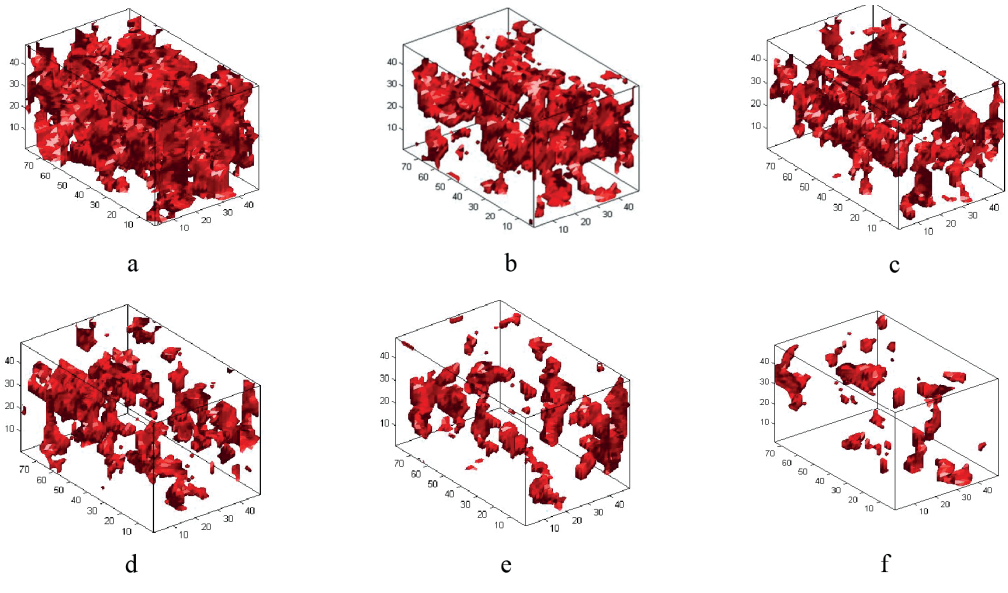

Fig. 6. Three-dimensional schematic diagram of residual oil morphology change at different oil saturation: a – 81.1%, b – 41.5%, c – 33.2%, d – 28.8%, e – 23.08%, f – 18.8%

The change in the three-dimensional shape of residual oil at different oil saturations is shown in Fig. 6, which demonstrates the morphology of residual oil during the displacement process.

Three cores with the same porosity and different permeability were selected to analyze the effect of permeability on the state of residual oil. The porosity of the studied cores C1, C2 and C3 are 37.6%, 38.5% and 39.5%, respectively, and the permeability is $1424 \cdot 10^{-3}$ μm², $2797 \cdot 10^{-3}$ μm² and $6288 \cdot 10^{-3}$ μm². The displacement rate was constant at 0.01 mL/min.

From Fig. 7 it follows that the more permeability of the core (the more connected pores), the more intensive continuous residual oil is transformed into other types of residual oil. If the permeability of the core is small, the range of filtering pores is also small and the oil displacement effect in the core is weak, the amount of residual oil is large and some amount of film residual oil also remains. When fully watered, the main type of residual oil in cores with different permeabilities is network residual oil. The 3D image of the morphology of residual oil at different permeabilities is shown in Fig. 8.

Conclusion

The proposed technology for studying the influence of reservoir microstructure on the morphology of residual oil is effective and due to its non-destructive control characteristics can be widely used to study the physical properties of the core, characterize the pore structure and study the filtration processes.

The combined application of one-dimensional NMR transverse relaxation spectrum with the traditional mercury injection method will make it possible to effectively study the structural size distribution of all pores. In the traditional method of studying the pore structure by mercury injection into the core, small-sized pores are not identified, which leads to a decrease in the informativeness of the method.

Calculation of permeability using NMR technology gives reliable results. With an adequate choice

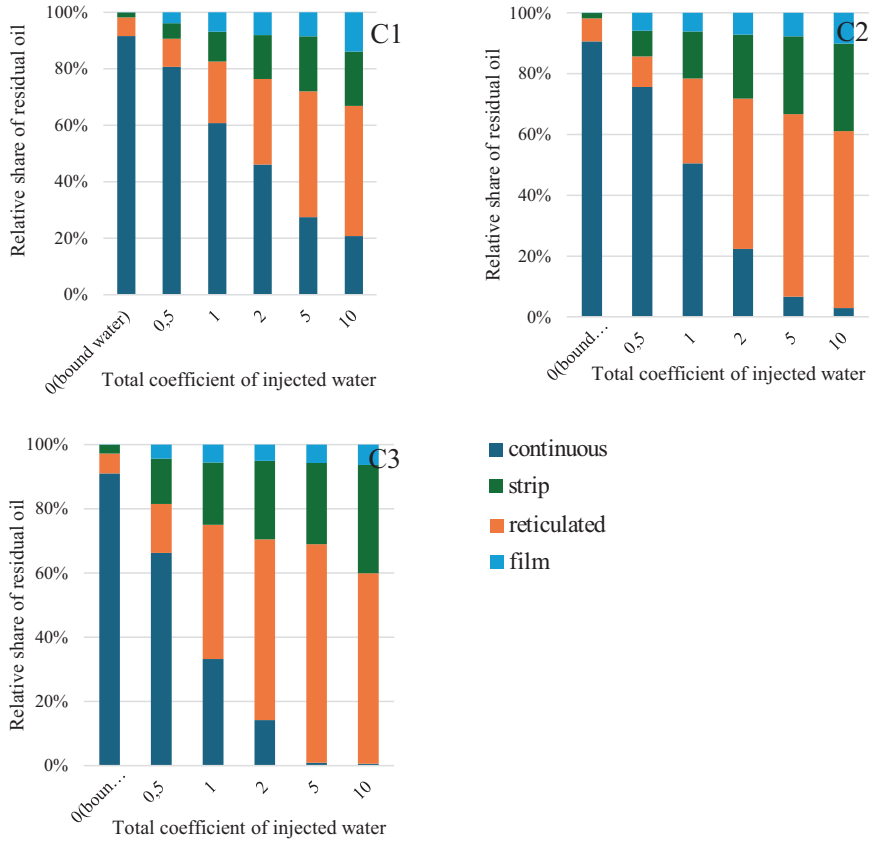

Fig. 7. Change in the relative share of residual oil of different types during waterflooding of cores with different permeability

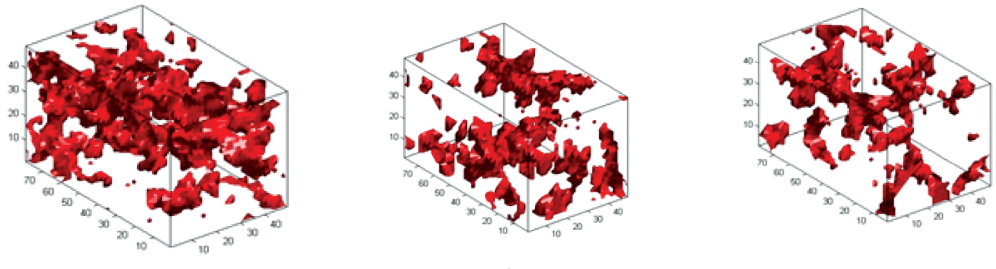

Fig. 8. 3D shapes of residual oil in cores with different permeability at the final stage of displacement: a – 1424·10⁻³ μm², b – 2797·10⁻³ μm², c – 6288·10⁻³ μm²

of interpretation model for calculating the absolute permeability of rocks, the NMR method allows to overcome the existing limitations of traditional methods.

Depending on the pore microstructure and microscopic state, four types of residual oil are distinguished: strip, film, reticulated and continuous.

References

Arns Ch.H. (2004). A comparison of pore size distributions derived by NMR and X-ray-CT techniques. *Physica A: Statistical Mechanics and Its Applications*, 339(1–2), pp. 159–165. https://doi.org/10.1016/j.physa.2004.03.033

Azizoglu Z., Garcia A.P., Newgord Ch., Heidari Z. (2020). Simultaneous Assessment of Wettability and Water Saturation Through Integration of 2D NMR and Electrical Resistivity Measurements. *SPE Annual Technical Conference and Exhibition*, SPE-201519-MS. https://doi.org/10.2118/201519-MS

Chen J., Hirasaki G.J., Flaum M. (2006). NMR wettability indices: Effect of OBM on wettability and NMR responses. *Journal of Petroleum Science and Engineering*, 52(1–4), pp. 161–171, https://doi.org/10.1016/j.petrol.2006.03.007

Coates G.R., Miller M., Gillen M., Henderson C. (1991). The MRIL In Conoco 33-1 An Investigation Of A New Magnetic Resonance Imaging Log. *SPWLA 32nd Annual Logging Symposium*, SPWLA-1991-DD.

Kenyon W.E. (1997). Petrophysical Principles of Applications of NMR Logging. *The Log Analyst*, 38(2), SPWLA-1997-v38n2a4.

Kenyon W.E., Day P.I., Straley C., Willemsen J.F. (1988). A Three-Part Study of NMR Longitudinal Relaxation Properties of Water-Saturated Sandstones. *SPE Formation Evaluation*, 3(3), pp. 622–636, https://doi.org/10.2118/15643-pa

Kleinberg R.L., Straley C., Kenyon W.E., Akkurt R., Farooqui S.A. (1993). Nuclear Magnetic Resonance of Rocks: T_1 vs. T_2. *SPE Annual Technical Conference and Exhibition*, SPE-26470-MS. ttps://doi.org/10.2118/26470-MS

Melekhin S.V., Mikhailov N.N. (2017) Laboratory modeling of residual oil mobilization in flooded reservoirs. *SPE Russian Petroleum Technology Conference*. SPE-187887-MS. https://doi.org/10.2118/187887-MS

Mikhailov N.N. (1992). Residual oil saturation of the developed formations. Moscow: Nedra, 272 p. (In Russ.)

Mikhailov N.N. (2011). Petrophysical support of new technologies for the recovery of residual oil from technogenically altered deposits. *Karotazhnik,* 7(205), pp. 126–137. (In Russ.)

Sulucarnain I., Sondergeld C.H., Rai C.S. (2012). An NMR Study of Shale Wettability and Effective Surface Relaxivity. All Days. *SPE Canadian*

Unconventional Resources Conference, SPE-162236-MS. https://doi.org/10.2118/162236-ms

Sun Zh., Jia L., Zhang L., Sun B., Zhang Y. (2017). Application of NMR Technology in Pore Structure Evaluation for Low-Permeability and Low-Viscosity Oil Reservoirs. *Xinjiang Petroleum Geology*, 38(6), pp. 735–739. https://doi.org/10.7657/XJPG20170617

Tchistiakov A.A., Shvalyuk E.V., Kalugin A.A.(2022). The rock typing of complex clastic formation by means of computed tomography and nuclear magnetic resonance. *Georesursy = Georesources*, 24(4), pp. 102–116. (In Russ.) https://doi.org/10.18599/grs.2022.4.9

Yan W., Sun J., Dong H., Cui L. (2021). Investigating NMR-based absolute and relative permeability models of sandstone using digital rock techniques. *Journal of Petroleum Science and Engineering*, 207, 109105. https://doi.org/10.1016/j.petrol.2021.109105

About the Authors

Mo Jiali – Graduate student, National University of Oil and Gas "Gubkin University"

Build. 1, 65, Leninsky ave., Moscow, 119991, Russian Federation

e-mail: mojiali111@gmail.com

Nikolai N. Mikhailov – Dr. Sci. (Technical Sciences), Professor, National University of Oil and Gas "Gubkin University"; Chief Researcher, Institute of Oil and Gas Problems of the Russian Academy of Sciences

Build. 1, 65, Leninsky ave., Moscow, 119991, Russian Federation

e-mail: folko200@mail.ru

Wang Hengyang – PhD (Technical Sciences), Associate Researcher, Sinopec Research Institute of Petroleum Engineering

197 Baisha Road, Beijing, 102206, China

e-mail: wanghengyang716@mail.com

Manuscript received 7 November 2023;
Accepted 19 February 2024;
Published 30 March 2024

IN RUSSIAN

Влияние микроструктуры коллектора на состояние остаточной нефти по данным релаксометрии ядерно-магнитного резонанса

Мо Цзяли[1], Н.Н. Михайлов[1,2], Ван Хэнян[3]*

[1]Российский государственный университет нефти и газа (национальный исследовательский университет) имени И.М. Губкина, Москва, Россия
[2]Институт проблем нефти и газа РАН, Москва, Россия
[3]Sinopec Научно-исследовательский институт нефтяной инженерии, Пекин, Китай
[*]Ответственный автор: Николай Нилович Михайлов, e-mail: folko200@mail.ru

Исследовано влияние свойств керна на состояние остаточной нефти в процессе вытеснения нефти водой на микроуровне. Рассмотрены распределение пор по размерам, проницаемость керна, динамика и морфология остаточной нефти. Анализ имеющихся экспериментальных подходов к изучению свойств керна и остаточной нефти в образцах показал, что существующие способы не дают полной информации об изучаемых параметрах. Для решения этих проблем предложено совместное использование инновационной технологии релаксационно-диффузионной релаксометрии ядерно-магнитного резонанса (ЯМР) с традиционной технологией. Для измерения долевого распределения пор по размерам использован комбинированный метод инжекции ртути и ядерного магнитного резонанса. С помощью метода ЯМР определена проницаемость керна. Двумерная ЯМР-релаксометрия позволяет изучать микроскопическое состояние остаточной нефти в ненарушенном керне в процессе вытеснения. С помощью предлагаемой методики исследован керн месторождения Шэнли в Китае. Получены распределения пор по размерам, определены проницаемость и остаточная нефтенасыщенность на разных стадиях вытеснения. Выделены четыре типа остаточной нефти: полосообразная (островная), пленочная, сетчатая, непрерывная. Показано влияние проницаемости на долевое содержание разных типов остаточной нефти в процессе вытеснения. Результаты исследований демонстрируют влияние структуры порового пространства и смачиваемости на состояние остаточной нефти.

Ключевые слова: типы остаточной нефти, структура порового пространства, релаксационно-диффузионная двумерная релаксометрия ядерно-магнитного резонанса

Для цитирования: Цзяли Мо, Михайлов Н.Н., Хэнян Ван (2024). Влияние микроструктуры коллектора на состояние остаточной нефти по данным релаксометрии ядерно-магнитного резонанса. *Георесурсы,* 26(1), с. 100–108. https://doi.org/10.18599/grs.2024.1.8